AIMS Geosciences, 2 (4): 329-344
DOI: 10.3934/geosci.2016.4.329
Received date 07 June 2016
Accepted date 08 November 2016
Published date 10 November 2016

http://www.aimspress.com/journal/geosciences

*Research article*

# Utilizing Vegetation Indices as a Proxy to Characterize the Stability of a Railway Embankment in a Permafrost Region

**Priscilla Addison [1,*], Pasi Lautala [2] and Thomas Oommen [1]**

[1] Department of Geological and Mining Engineering and Sciences, Michigan Technological University, Houghton, MI-49931, USA
[2] Department of Civil Engineering, Michigan Technological University, Houghton, MI-49931, USA

*** Correspondence:** Email: peaddiso@mtu.edu; Tel: +1-810-620-0495

**Abstract:** Degrading permafrost conditions around the world are posing stability issues for infrastructure constructed on them. Railway lines have exceptionally low tolerances for differential settlements associated with permafrost degradation due to the potential for train derailments. Railway owners with tracks in permafrost regions therefore make it a priority to identify potential settlement locations so that proper maintenance or embankment stabilization measures can be applied to ensure smooth and safe operations. The extensive discontinuous permafrost zone along the Hudson Bay Railway (HBR) in Northern Manitoba, Canada, has been experiencing accelerated deterioration, resulting in differential settlements that necessitate continuous annual maintenance to avoid slow orders and operational interruptions. This paper seeks to characterize the different permafrost degradation susceptibilities present at the study site. Track geometry exceptions were compared against remotely sensed vegetation indices to establish a relationship between track quality and vegetation density. This relationship was used as a proxy for subsurface condition verified by electrical resistivity tomography. The established relationship was then used to develop a three-level degradation susceptibility chart to indicate low, moderate and high susceptibility regions. The defined susceptibility regions can be used to better allocate the limited maintenance resources and also help inform potentially long-term stabilization measures for the severely affected sections.

**Keywords**: Site characterization; permafrost; remote sensing; track geometry; electrical resistivity; degradation susceptibility; NDVI

## 1. Introduction

Statistics gathered from the Federal Railway Administration (FRA) showed that 70% of all train accidents in 2015 in the U.S. were caused by derailments [1]. One of the most significant derailment causes include defects in track geometry, as trains have very low tolerances to vertical and horizontal imperfections [2]. Railway embankments located in permafrost regions globally are becoming more vulnerable to such occurrences due to accelerated permafrost degradation [3–7]. Permafrost degradation results in the formation of differential settlements, which can then potentially cause track geometry defects resulting in derailments.

Permafrost is defined as "ground that remains at or below 0 ℃ for at least two consecutive years for natural climatic reasons" [8]. Depending on the extent of the subsurface that is underlain by permafrost, three different permafrost types can be defined:

- *Continuous Permafrost*: 90 to 100% of the subsurface is underlain by permafrost, with the permafrost being only absent under deep bodies of water which do not fully freeze to the bottom in winter [8];
- *Extensive Discontinuous Permafrost*: 50 to 90% of the subsurface is underlain by permafrost [8]; and
- *Sporadic Discontinuous Permafrost*: Less than 50% of the subsurface is underlain by permafrost [8].

This study focused on the Hudson Bay Railway (HBR), a 510-mile track constructed within the permafrost region of northern Manitoba, Canada. The HBR, owned by OmniTRAX Inc. at the time of this study, serves as a critical linkage for passengers and freight from The Pas (milepost 0) to Churchill (milepost 510), connecting locations in North America to international destinations through the Port of Churchill. All three permafrost types occur along the HBR route. From The Pas to Churchill, there is a gradual northward transition from no permafrost zone, to sporadic discontinuous, to extensive discontinuous, and finally to continuous permafrost (Figure 1).

In response to an increasingly warming climate, the HBR has been experiencing differential settlements within its discontinuous permafrost zones during thawing summer seasons since the completion of the line in 1929. These differential settlements, termed "sinkholes," have been found to develop in response to thawing of the underlying warm, ice-rich permafrost soils within the subgrade. Sinkholes mainly form in the discontinuous permafrost zones at transitions between no permafrost (fen) to permafrost ground (peat plateau), as the relatively warm fen loses its heat to the adjacent relatively cold peat plateau. Short sections of track that overlay these activated sinkholes may experience as much as 15 cm (five inches) of settlement during a single summer thawing season [9].

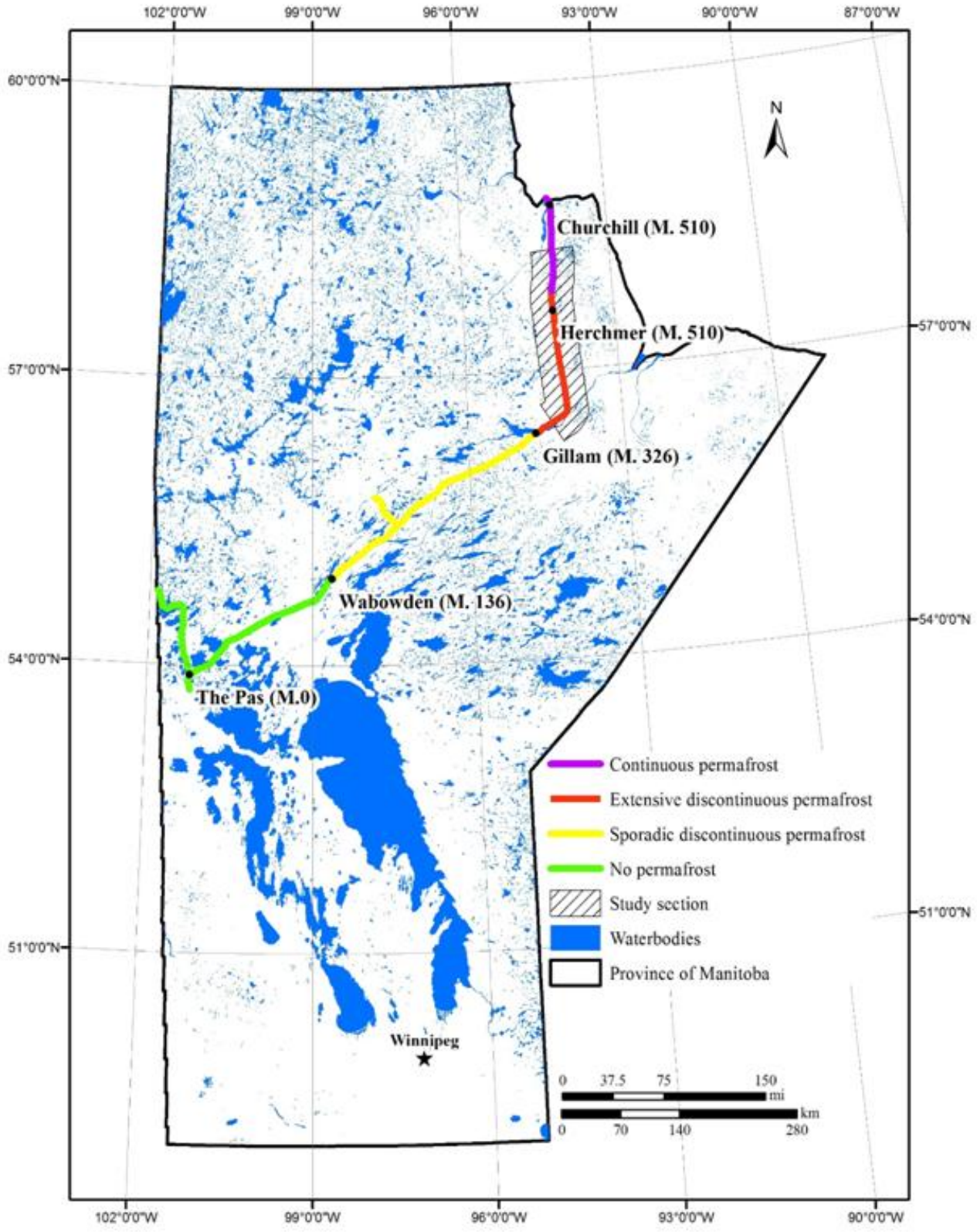


**Figure 1. Location of the HBR from The Pas to Churchill showing the varying permafrost conditions.**

To subvert the effect of sinkholes and keep the track safe and operational, extensive and frequent resurfacing with ballast is performed annually. Currently, maintenance is performed on as-needed basis. However, railway owners are interested in developing a data-driven understanding of the corridor conditions that can be used to effectively allocate limited maintenance resources and plan for long-term stabilization measures for severely affected sections. In a bid to address this challenge, this paper offers a first step toward a solution by characterizing the railway embankment and identifying different permafrost degradation severities along the HBR. Rather than using the traditional method of borehole drilling for characterization, which is time consuming and costly, this research proposes an integration of three technologies as a more rapid and economic method.

The proposed methodology involves employing an integration of track geometry analyses, remote sensing techniques, and geophysical profiling as investigative tools. More specifically, records of track geometry exceptions data were compared against remotely-sensed vegetation indices to establish a relationship between track quality and vegetation density, as past studies have shown vegetation pattern to have a strong influence on the relative intactness of permafrost [10,11]. Electrical resistivity tomography was then used to validate that the vegetation density and track quality indeed provided an accurate picture of the subsurface permafrost conditions.

## 2. Methodology

### *2.1. Study Area*

Since the completion of the HBR in 1929, sinkhole formation has been an increasingly recurrent phenomenon during the summer thawing season. From 1976–1991, an engineering consulting company, EBA Engineering Consultants Limited (from here onwards referred to as EBA), was tasked to undertake extensive research along the rail corridor to understand the geothermal regime of the subsurface and to uncover the mechanism of sinkholes formation [9]. The reports produced by EBA indicate that the extensive discontinuous permafrost region between mileposts 330 and 430 is the most problematic segment of the HBR [12,13]. Recent track surfacing records, increases in slow orders (speed restrictions placed on a section of track to limit train speeds below regular limits due to unfavourable track conditions) [14], and interviews with OmniTRAX personnel confirmed that this section remains the most problematic, depicting increasing structural instability. Hence this section of the HBR, as well as an overlap in the continuous permafrost region to milepost 473, was chosen as the focus of the study (Figure 1).

### *2.2. Data Analyses*

The following sections give brief backgrounds on the three individual techniques used—track geometry analyses, geophysical exploration, and remote sensing analyses. The last section describes how all three techniques were integrated for the route characterization study.

### *2.3. Track Geometry Analyses*

The term *track geometry* refers to the measured relative positions of the different geometrical elements—profile, gauge, alignment, crosslevel, warp, etc. [15]—along a railway track in space and time [16]. Transportation authorities in different countries set maximum permissible thresholds for each of these different elements for a given set of traffic and operating conditions. All railway tracks across the country have to conform to such standards to be considered safe for operations. The HBR follows the standards set by Transport Canada.

Track geometry measurements may be obtained either through manual inspections or automated data collection by specialized vehicles. Manual inspections involve trained personnel using approved methods to take measurements of the various geometry elements of the track. This is time consuming and is usually only conducted at locations with noticeable deviations from track standards. Automated data collection, on the other hand, is a technique where a vehicle operating on rails, uses either laser or mechanical gauges, to take uniform and continuous measurements of the different geometry parameters as it travels along the corridor. The measurements also indicate locations where geometry deviations exceed or approach the limits allowed in approved standards. These tagged locations are known as *track exceptions* or *track defects*. In this paper, they are referred to as *track exceptions*.

The automated vehicle acquisition is the method used along the HBR to collect continuous data at one-foot intervals. Three complete sets of geometry survey data, one each, from 2012, 2013 and 2014, were obtained and used to extract track exception data with Andian Technologies' GeoPrint 3.30 software [17] for further analyses.

### *2.4. Geophysical Investigation*

Electrical resistivity tomography (ERT) is the geophysical method that was adopted for the research. This method is known to work particularly well in permafrost areas [18–21]. ERT functions on the principle that different materials offer varying resistance to the flow of current, a property known as the material's resistivity. Water resistivity increases strongly at the freezing point due to the phase change from electrically conductive water to electrically non-conductive ice [22]. This intrinsic quality is what makes it easy to differentiate frozen permafrost table (high resistivity) from thawed saturated active layer lying on top of it (low resistivity).

Two sets of ERT field data collections were taken: one during October 2014 and a second during September 2015. The collections were scheduled during the fall season, when the top layer of soil was fully thawed, to allow for a clear delineation of the permafrost profile. A total of 10 sites were selected, mainly to match locations with borehole and geophysical data from EBA's past work, as it facilitated comparison between current and previous results. The SuperSting 2D multi-electrode system [23] was the instrumentation used for the ERT survey. At each test location, 28 electrodes were inserted into the ground at equal distances. Current was injected into the ground and a set of apparent resistivity values were measured by the electrodes, producing a 2D dataset along the profile. Acquired data was analyzed with Advanced Geosciences, Inc.'s EarthImager 2D inversion and modelling software [24] using a smooth model inversion. Results from this study were compared to spatially corresponding track exception data for the 10 sites to assess the trends between the two datasets. The objective was to infer subsurface conditions delineated by the ERT with the surficial data of the track geometry exceptions.

### *2.5. Remote Sensing of Vegetation Pattern*

Vegetation has been identified as one of the key factors that influences the relative intactness of permafrost [25,26]; thus, changes in vegetation density have greater effect on the degradation or aggradation of permafrost than fluctuations in climatic regime [27]. A typical permafrost ecosystem has a thick and spongy mossy vegetation on top of it. The moss layer acts as an insulating mat that traps stagnant air to reduce the thermal contact between air and ground during the summer months. In addition to its insulating properties, the organic mat also cools the ground through the process of evaporation. Lastly, typical tree cover found within permafrost regions, such as *Picea mariana* (black spruce) and *Picea glauca* (white spruce), shroud the ground from the radiant heat of direct sunlight and thereby retard/prevent permafrost thaw. Since higher vegetation density was believed to depict a more protected/intact permafrost, it was also expected to correlate with higher level of track quality, i.e. locations that record lower track exceptions within the study area. Vegetation density was therefore used as a proxy for the relative intactness of permafrost.

Satellite remote sensing was employed in this analysis as it offers a cost-effective quantitative approach to analyse the entire study area. The investigative period was limited to 2012–2014 to correspond to the available track geometry data. Data from only Landsat 8 (commissioned in 2013) was used since data from Landsat 7 was unusable due to its scan line corrector failure since May 2003 [28]. Pre-requisites for scenes used for the investigation were that they had to be from the summer season since the vegetation is at the peak of the growing season and the ground is snow-free. The scenes also had to be cloud-free to prevent erroneous estimations from cloud contamination. Landsat 8's scene from row 31, path 20 acquired in July 29, 2014 is the only one that met these selection criteria. Although this data is from a single time stamp, the authors believe it is still representative of site conditions because in the relatively short investigative period of 2012–2014, no

extreme environment-altering phenomena such as wildfires occurred, leading to the hypothesis that the plant communities within the study site remained the same throughout the three-year investigative period. The data was downloaded as a geometrically and radiometrically corrected Level 1 product. It was first converted to radiance and then to top-of-atmosphere (TOA) reflectance, using the steps outlined by Chander et al. [29]. To analyze vegetation condition (i.e., differentiate between "normal" growing conditions and stressed), Normalized Differenced Vegetation Index (NDVI) was calculated using the TOA image after Rouse et al. [30].

### *2.6. Integration of Methods*

Results from the ERT surveys at the 10 sites were compared against the track exception data to identify trends between these datasets. The objective was to infer subsurface conditions delineated by the ERT from the surficial data of the track exceptions. After establishing this relationship, the NDVI from the remote sensing analyses was compared against their corresponding average number of track exceptions recorded. This analysis was modelled after Roghani et al.'s approach [31] by dividing the study section into 22-mile sections, resulting in six subsections from milepost 341 (southern end) to milepost 473 (northern end). The process is summarized in Figure 2. The corresponding track exceptions per mile of track were calculated by combining the recorded yearly average exceptions per section and dividing them by the segment length (22-miles).

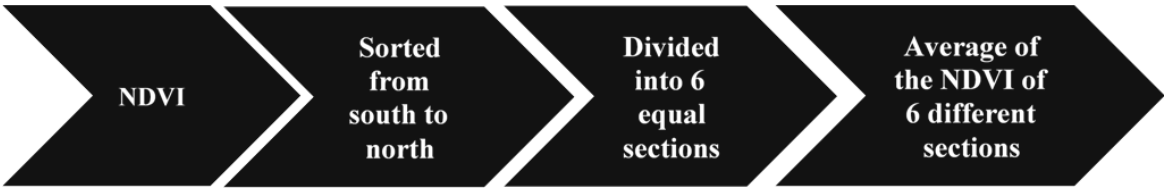


**Figure 2. Process for determining relation between NDVI and track geometry exceptions.**

## 3. Results and Discussion

### *3.1. Relationship between Track Geometry Exceptions and Subsurface Profile*

A plot of the six subsections against their recorded average geometry exceptions indicated a general increasing trend in exceptions from subsection 1 to 6 (Figure 3) which confirms worsening track conditions from south to north.

Results of the subsurface profiles from the ERT investigation are displayed along a plot of the study section in Figure 4. The legend at the bottom right of the figure provides an explanation of the color scheme from blue to red, representing low to high resistivities. Palacky and West [32] found that the average resistivity for permafrost materials is 10,000 ohm. Figure 4 shows that several

locations recorded a resistivity of 10,000 ohm indicating the presence of permafrost (indicated by the red color).

From Figure 4, it can be seen that the only site underlain by well-defined continuous permafrost is milepost 382. For all other sites, various degrees of permafrost degradation were observed. Particularly noteworthy is that excluding the subsurface profile of milepost 363, the southern sections of the study area were found to be almost devoid of permafrost. The lack of permafrost in the southern sections correlate with lower records of track exceptions in the south as observed in Figure 3. The northern sections, which recorded higher track exceptions, have permafrost present but they seem to be actively thawing, as indicated by the profusion of thawing transition zones. These subsurface profiles suggest that permafrost zones classification by EBA (shown in Figure 1) is changing, as permafrost degradation appears to be moving northward. It is likely that the southern boundary of the extensive discontinuous permafrost zone is transitioning into a sporadic discontinuous zone, whereas the southern boundary of the continuous permafrost zone may also be converting into extensive discontinuous zone. The results also confirm EBA's hypothesis that sinkholes develop at the permafrost transition zones, as thawing northern sections with the most transition zones also recorded the high occurrences of track exceptions.

Based on these analyses, it can be concluded that locations with high track geometry exceptions are likely underlain by thawing permafrost and locations with few or no track exceptions are mostly devoid of permafrost. With this relationship established, the next step was to discern the relationship between track exceptions and vegetation trends.

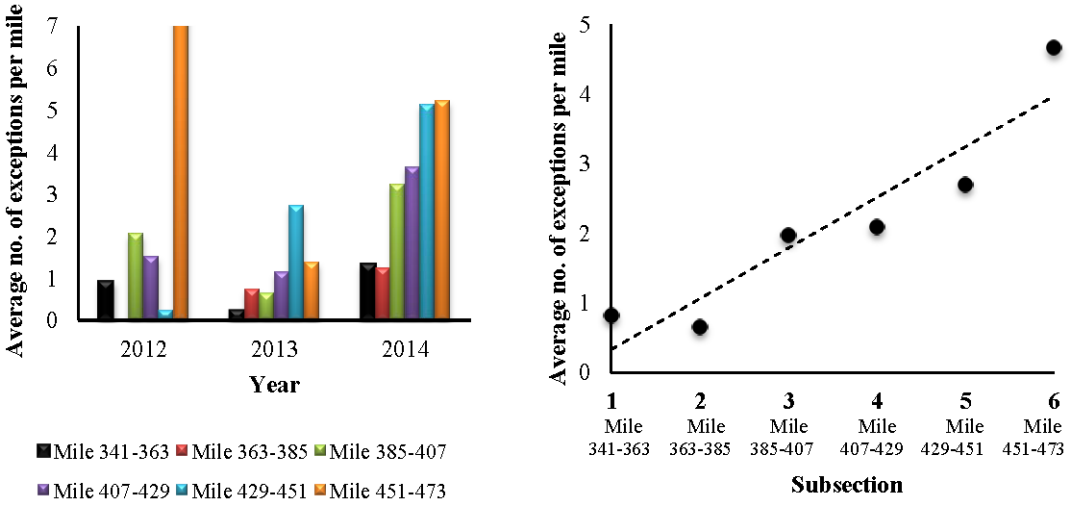


**Figure 3. A plot of track exceptions recorded for the six subsections in 2012–2014 (left); and a plot of the average track exception recorded for the investigative period for each subsection (right).**

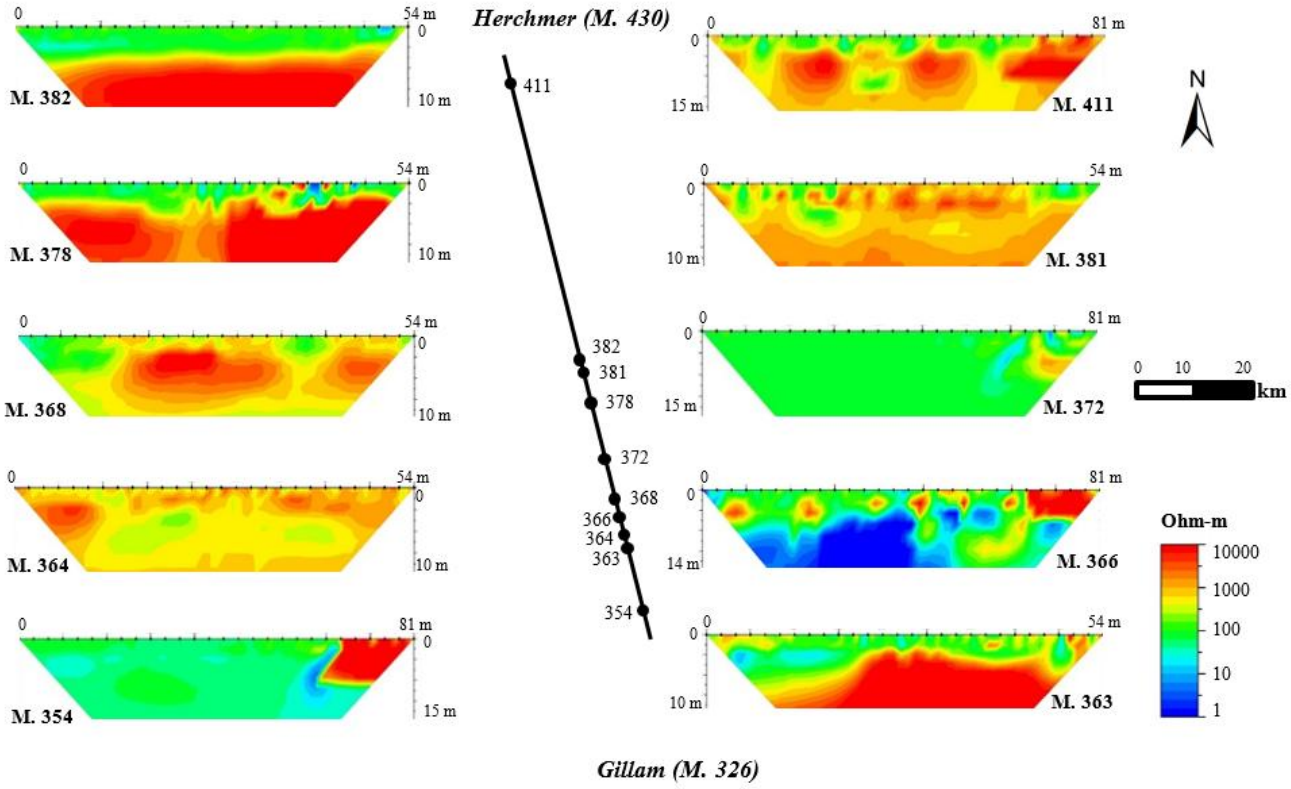


**Figure 4. Subsurface profiles from the ERT investigation displayed along the track route of the study section, showing ground resistivities from low resistive thawed soils in blue to highly resistive permafrost layers in red color.**

### *3.2. Relationship between Vegetation and Exceptions*

NDVI was compared against the corresponding average number of track exceptions recorded for each of the six subsections. A plot of the NDVI against subsection shows a general negative correlation from section 1 to 6 (Figure 5A), which indicates a decrease in the vegetation density as one moves northward. A plot of the NDVI versus the track exception also shows a negative correlation indicating that as vegetation decreases, the number of track exceptions increases and vice versa (Figure 5B).

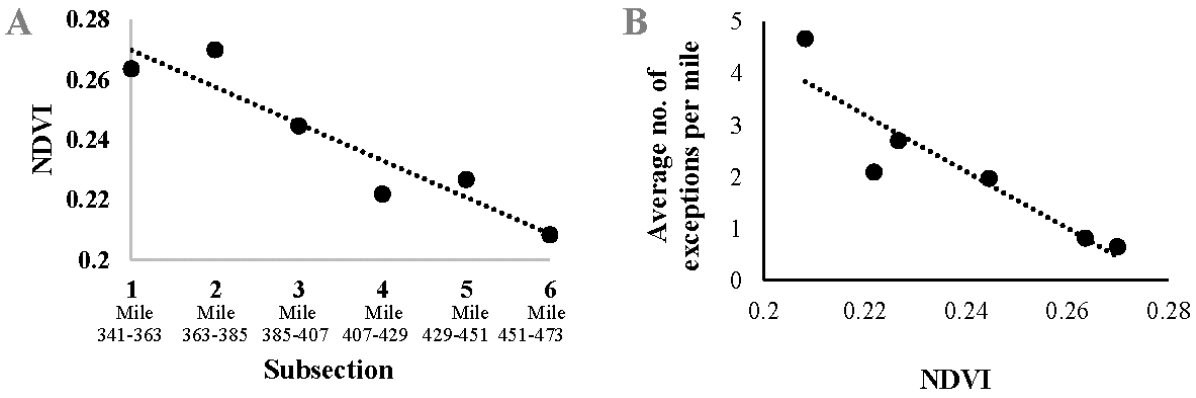


**Figure 5. A plot of track sections versus NDVI showing the tendency to find less vegetation as you move northwards (left); and NDVI versus track exceptions showing that it is more likely to find track exceptions in locations with little vegetation and vice versa (right).**

Photo images were taken in 10-second intervals while traversing the entire study area by a hi-rail truck. A comparison between the photos and research findings revealed that the northernmost sections with the lowest NDVIs (Subsections 5 and 6) are generally devoid of tree cover. This is intuitive; however, a more noteworthy finding was that these sections had substantial amounts of ponded surface water close to the embankment shoulders. Figure 6 shows two such typical images for milepost 468 (Subsection 5) and milepost 448 (Subsection 6). Conversely, the southernmost sections, which recorded the highest NDVIs, had denser vegetation with no surface water close to the embankment shoulders (Figure 7). From these photos, it was realized that the low NDVIs obtained for this particular study site translate not only to low vegetation densities but also to high percentage of ponded surface water.

**Figure 6. Photos of milepost 468 (left) and milepost 448 (right) showing no tree cover and ponded water close to embankment shoulders.**


**Figure 7. Photos of milepost 349 (left) and milepost 377 (right) showing population of trees and no surface water ponded close to the embankment shoulders.**

These photos also reinforced the perceived relationship between the NDVI and track exceptions, as past literature have shown collected waterbodies in the form of ponds and lakes have deleterious effects on underlying permafrost. Ponded water absorbs the sun's heat and transfers it to the permafrost table [33], which explains why the northernmost sections recorded higher frequencies of track exceptions, indicative of permafrost degradation.

### *3.3. Degradation Susceptibility Chart*

As the fundamental aim of this study was to characterize the permafrost degradation susceptibility along the HBR, the established relationship between the NDVI and track exceptions was used to develop a degradation susceptibility chart. The chart was developed to delineate sections in the extensive discontinuous permafrost zone that will require additional maintenance attention and those that will not. It should be noted that the defined classifications are empirical and are based on parameters specific to the extensive discontinuous permafrost zone of the HBR. Any adaption of the methodology to other sites requires site specific analyses.

The average number of exceptions recorded was used as the basis of the chart. Locations that developed a maximum of one exception per year were generally considered stable and within acceptable performance levels, whereas locations that developed more than 2.5 exceptions are of concern and need to be mitigated [31]. Using these two track exception limits, a three-level severity chart was developed. The results are summarized in Figure 8 and Table 1.

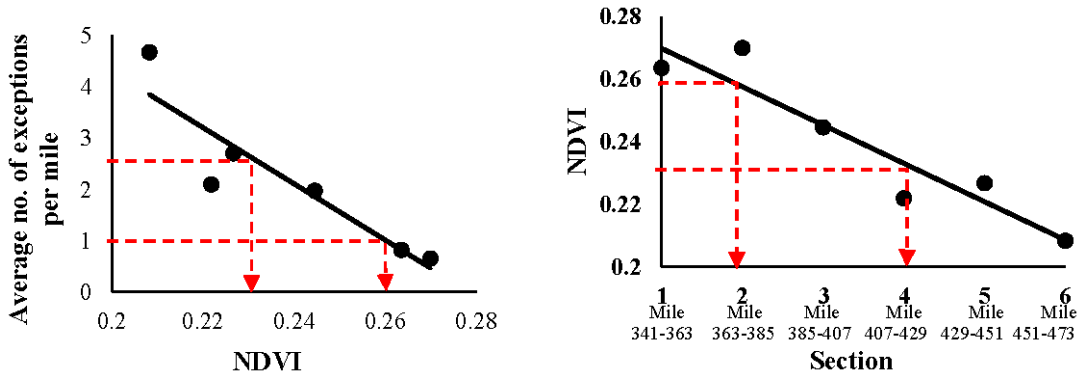


**Figure 8. Defining percentiles for developing severity chart.**

**Table 1. Permafrost degradation susceptibility chart developed for study section along the HBR.**

| Rating | Degradation Susceptibility | Vegetation | Exceptions | Mileposts |
|---|---|---|---|---|
| **1** | Low | **NDVI** > 0.26 | **E** < 1 | **341–363** |
| **2** | Moderate | 0.23 ≤ **NDVI** ≥ 0.26 | 2.7 ≤ **E** ≥ 1 | 363–407 |
| **3** | High | **NDVI** < 0.23 | **E** > **2.7** | **407–473** |

A rating of 1 represents a low degradation susceptibility region, located between mileposts 341 and 363. This region is predicted to develop no more than one track exception per mile annually and is characterized by having continuous vegetation and no ponded surface water, with an NDVI of 0.26 or higher. The region can be inferred as being the least susceptible to permafrost degradation due to the fact that it is likely underlain by a thawed subsurface or a stable intact permafrost.

A rating of 2 represents a medium degradation susceptibility region, located between mileposts 363 and 407. This region is predicted to develop between 1 to 2.5 track exceptions per mile annually, with an NDVI between 0.23 and 0.26.

A rating of 3 represents the northernmost extent of high degradation susceptibility, located between mileposts 407 and 473. This region is predicted to develop at least 2.5 track exceptions per mile every year and is characterized by having sparse vegetation with water ponded close to the embankment shoulders, and an NDVI of 0.23 or lower. The region can be inferred as being most susceptible to permafrost degradation due to the fact that it is likely underlain by an actively thawing permafrost table with many transition zones.

## 4. Conclusions and Future Work

This study looked into using innovative methods to characterize permafrost degradation susceptibility along the deteriorating railway embankment of the Hudson Bay Railway (HBR) in northern Manitoba, Canada. A combination of track geometry analyses, geophysical explorations, and remote sensing techniques was used to locate and delineate the severity of the different stability challenges found along the HBR.

The analyses revealed that locations with high records of track geometry exceptions are likely underlain by thawing permafrost, whereas locations with low geometry exceptions tend to be devoid of permafrost. A comparison of the track exceptions against NDVI confirmed that locations with low NDVI have high records of track exceptions, which is indicative of permafrost degradation. The converse was found to also hold true.

Photo surveys taken at the study site revealed that for the HBR corridor, low NDVI does not only translate to the typical interpretation of low vegetation density, but more importantly, to an accumulation of ponded water close to the embankment shoulders. These photos also reinforced the perceived relationship between NDVI and track exceptions, as past literature concluded surface water to have a detrimental effect on the underlying permafrost. This study confirmed that ponded water is an important contributor to the permafrost degradation found along the HBR.

The established relationships were used to develop a three-level permafrost degradation susceptibility chart with ratings of 1, 2, and 3 representing low, moderate and high susceptibility regions, respectively. The chart was developed to delineate sections in the study area that need more frequent maintenance attention and represents a first step towards developing a data-based approach to maintenance activities for the HBR. The defined susceptibility regions can be used to more strategically allocate limited maintenance resources and narrow down the consideration of long-term stabilization measures for segments that are more severely affected.

The study also illustrated that earlier permafrost zone classifications by EBA may be shifting, as permafrost degradation was seen to be moving northward. It is likely that lower boundary of the extensive discontinuous permafrost zone is evolving into a sporadic discontinuous zone, and the lower boundary of the continuous permafrost zone may also be transitioning into an extensive discontinuous zone. Future work should refine these current boundaries.

## Acknowledgments

This research was made possible by the financial support of OmniTRAX Inc. and National University Rail (NURail) Center funded by the U.S Department of Transportation, Research and Innovative Technology Administration (USDOT-RITA).

## Conflict of Interest

All authors declare no conflicts of interest in this paper.

## References


1. Admnistration FR (2015) Accident Trends—Summary Statistics. Available from: http://safetydata.fra.dot.gov/officeofsafety/publicsite/graphs.aspx, [accessed 2015].
2. Peng F, Kang S, Li X, et al. (2011) A heuristic approach to the railroad track maintenance scheduling problem. *Comput-Aided Civ Infrastruct Eng* 26: 129-145.
3. Jorgenson MT, Harden J, Kanevskiy M, et al. (2013) Reorganization of vegetation, hydrology and soil carbon after permafrost degradation across heterogeneous boreal landscapes. *Environ Res Lett* 8: 035017.
4. Jorgenson MT, Racine CH, Walters JC, et al. (2001) Permafrost degradation and ecological changes associated with a warmingclimate in central Alaska. *Clim change* 48: 551-579.
5. Osterkamp T (2007) Characteristics of the recent warming of permafrost in Alaska. *J Geophys Re: Earth Surf* 112.
6. Osterkamp T, Jorgenson M, Schuur E, et al. (2009) Physical and ecological changes associated with warming permafrost and thermokarst in interior Alaska. *Permafr Periglac Process* 20: 235-256.
7. Racine CH, Walters JC (1994) Groundwater-discharge fens in the Tanana Lowlands, interior Alaska, USA. *Arct Alp Res* 418-426.
8. Van Everdingen RO (1998) Multi-Language Glossary of Permafrost and Related Ground-Ice Terms in Chinese, English, French, German, Icelandic, Italian, Norwegian, Polish, Romanian, Russian, Spanish, and Swedish: International Permafrost Association, Terminology Working Group.
9. Ltd. EEC (1977) Settlement of a Railway Embankment Constructed on Permafrost Peatlands. Engineering report prepared for Canadian National Railways.
10. Chasmer L, Quinton W, Hopkinson C, et al. (2011) Vegetation canopy and radiation controls on permafrost plateau evolution within the discontinuous permafrost zone, Northwest Territories, Canada. *Permafr Periglac Process* 22: 199-213.
11. Zhang T, Barry RG, Armstrong RL (2004) Application of satellite remote sensing techniques to frozen ground studies. *Polar Geogr* 28: 163-196.
12. Ltd. EEC (1990) Prototype Stability Program, Hudson Bay Railway. Engineering report prepared for Canadian National Railways.
13. Addison PE, Oommen T, Lautala P (2015) A Review of Past Geotechnical Performance of the Hudson Bay Rail Embankment and Its Comparison to the Current Condition. American Society of Mechanical Engineers. pp. V001T001A033-V001T001A033.

14. Addison PE, Lautala P, Oommen T, et al. (2016) Embankment Stabilization Techniques for Railroads on Permafrost. American Society of Mechanical Engineers. pp. V001T01A008-V001T01A008.
15. Safety OoR (2014) Track and Rail and Infrastructure Integrity Compliance Manual. In: USDOT, editor: Federal Railroad Administration.
16. Zarembski AM, Palese JW (2006) Managing risk on the railway infrastructure. pp. 4-8.
17. Andian (2016) GoePrint. Available from: http://www.andian.com/?page=products&section=geoprint, [accessed October 07, 2016].
18. Douglas TA, Jorgenson MT, Brown DR, et al. (2015) Degrading permafrost mapped with electrical resistivity tomography, airborne imagery and LiDAR, and seasonal thaw measurements. *Geophysics* 81: WA71-WA85.
19. Hubbard SS, Gangodagamage C, Dafflon B, et al. (2013) Quantifying and relating land-surface and subsurface variability in permafrost environments using LiDAR and surface geophysical datasets. *Hydrogeol J* 21: 149-169.
20. Kneisel C, Emmert A, Kästl J (2014) Application of 3D electrical resistivity imaging for mapping frozen ground conditions exemplified by three case studies. *Geomorphol* 210: 71-82.
21. Lewkowicz AG, Etzelmüller B, Smith SL (2011) Characteristics of discontinuous permafrost based on ground temperature measurements and electrical resistivity tomography, southern Yukon, Canada. *Permafr Periglac Process* 22: 320-342.
22. Kneisel C (2006) Assessment of subsurface lithology in mountain environments using 2D resistivity imaging. *Geomorphol* 80: 32-44.
23. AGI (2016) SuperSting Wi-F.i. Available from: https://www.agiusa.com/supersting-wi-fi, [accessed October 07, 2016].
24. AGI (2016) AGI EarthImager 2D. Available from: https://www.agiusa.com/agi-earthimager-2d, [accessed October 07, 2016].
25. Smith MW (1975) Microclimatic influences on ground temperatures and permafrost distribution, Mackenzie Delta, Northwest Territories. *Can J Earth Sci* 12: 1421-1438.
26. Williams D, Burn C (1996) Surficial characteristics associated with the occurrence of permafrost near Mayo, Central Yukon Territory, Canada. *Permafr Periglac Process* 7: 193-206.
27. Smith M, Riseborough D (1983) Permafrost sensitivity to climatic change. pp. 1178-1183.
28. Markham BL, Storey JC, Williams DL, et al. (2004) Landsat sensor performance: history and current status. *IEEE Trans Geosci Remote Sens* 42: 2691-2694.
29. Chander G, Markham BL, Helder DL (2009) Summary of current radiometric calibration coefficients for Landsat MSS, TM, ETM+, and EO-1 ALI sensors. *Remote Sens environ* 113: 893-903.
30. Rouse Jr JW, Haas R, Schell J, et al. (1974) Monitoring vegetation systems in the Great Plains with ERTS. *NASA Spec Publ* 351: 309.

31. Roghani A, Macciotta R, Hendry M (2015) Combining Track Quality and Performance Measures to Assess Track Maintenance Requirements. American Society of Mechanical Engineers. pp. V001T001A009-V001T001A009.
32. Palacky G, West G (1987) Electromagnetic methods in applied geophysics. *Resist Charact Geol Targets* 52-129.
33. Jorgenson MT, Romanovsky V, Harden J, et al. (2010) Resilience and vulnerability of permafrost to climate change This article is one of a selection of papers from The Dynamics of Change in Alaska's Boreal Forests: Resilience and Vulnerability in Response to Climate Warming. *Can J For Res* 40: 1219-1236.


AIMS Press